Supporting Information：

Calcium Alginate Gel Beads Containing Gold Nanobipyramids for Surface-Enhanced Raman Scattering Detection in Aqueous Samples

Jiaming Chen[†, §], *Yuanyuan Yang*[†, §], *Bingyong Lin*[‡], *Xueju Wei*[†]*, *Zhenyu Lin*[‡]*, *and Guolin Hong*[†]*

[†] Department of Laboratory Medicine, The First Affiliated Hospital of Xiamen University, Xiamen Key Laboratory of Genetic Testing, Xiamen, Fujian 361005, China;

[‡] College of Chemistry, Fuzhou University, MOE Key Laboratory for Analytical Science of Food Safety and Biology, Fujian Provincial Key Laboratory of Analysis and Detection Technology for Food Safety, Fuzhou, Fujian, 350116, China

*E-mail: xuejuwei@126.com (Xueju Wei);
*E-mail: zylin@fzu.edu.cn (Zhenyu Lin);
*E-mail: 18860089899@139.com (Guolin Hong)

Table of Content:

Calculation of the analytical enhancement factor (AEF)

The SERS analytical enhancement factor (AEF) was calculated according to the following equation:[1-3]

$$AEF = \left(\frac{I_{SERS}}{I_{NRS}}\right)\left(\frac{C_{NRS}}{C_{SERS}}\right)$$

where I_{SERS} and I_{NRS} are the integrated intensities at 1363 cm^{-1} obtained by SERS and normal Raman scattering (NRS) spectrum. I_{SERS} is 8204.7, and I_{NRS} is 301.9. C_{SERS} and C_{NRS} stand for the concentration of R6G solution used for SERS and normal Raman scattering measurements, 10^{-6} M and 0.1 M, respectively. As a result, the calculated AEF of proposed Au NBPs/CAGB is about 2.7×10^{6}.

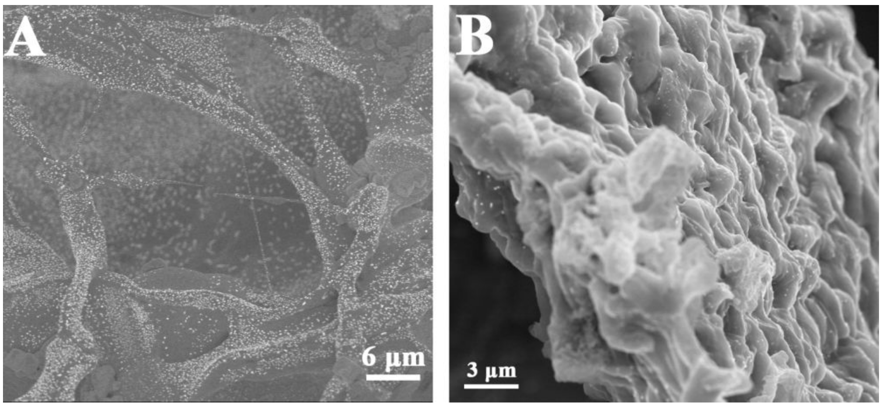

Figure. S1 (A) The SEM image of the Au NBPs/CAGB in large-scale. (B) The SEM image of the partial enlargement of a shrank and wrinkled cross section of Au NBPs/CAGB.

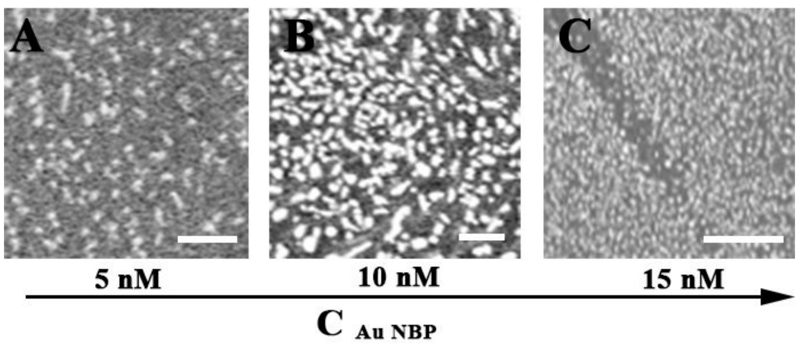

Figure. S2 SEM images of Au NBPs/CAGB cross section with different concentrations of Au NBPs: (A) 5 nM, (B) 10 nM, (C) 15 nM..

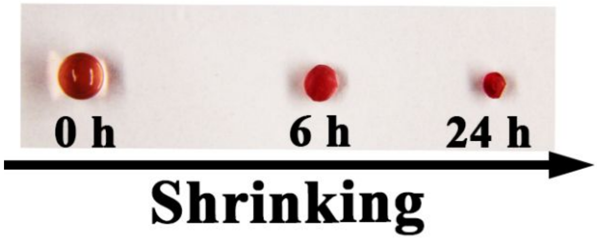

Figure. S3 The photographs of Au NBPs (10 nM)/CAGB exposed to environment (25°C, Relative humidity 60%). The volume of bead decreased with the time increasing.

Table S1. Experimental and Reported Raman Vibrational Modes and Assignments of Rhodamine 6G (cm^{-1})

Vibrational description	Rhodamine 6G	
	Observed	Reported[1, 4]
C-C-C ring in plane bending	613	613
C–H out of plane bending	777	775
Aromatic C-C stretching	1190	1183
Aromatic C-C stretching	1315	1312
Aromatic C-C stretching	1363	1364
Aromatic C-C stretching	1510	1512

Table S2. Comparison of the Performance of the Different SERS Platforms (Rhodamine 6G)

SERS platform	Detection method and time	RSD	Detection Range	LOD	Ref.
		Rhodamine 6G			
Graphene/Ag-nanoflowers/PMMA	Immersed into aqueous sample, 10 minutes	N.A.	10 fM ~ 1.0 nM	10 fM	6

Ag-nanosheet-grafted polyamide-nanofibers	Immersed into aqueous sample, 2 hours	<15%	0.01 nM ~ 10 nM	0.01 nM	[7]
Au nano-islands	Drop-casting, N.A.	N.A.	1.0 nM ~ 1.0 mM	1.0 nM	[8]
Cu-Ag layered periodic nanostructure	microfluidic, N.A.	8.8%	1.0 nM ~ 10 μM	1.0 nM	[9]
Roughened nano-Au film	N.A. & N.A.	<11%	1.0 nM ~ 10 μM	0.07 nM	[10]
Vertically-aligned Au NRs assembled at liquid–liquid interface	Direct measure of liquid-liquid interface, N.A.	N.A.	1.0 nM ~ 10 μM	1.0 nM	[11]
Superhydrophobic Ag coated taro leaf	Drop-casting, ~2 hours	9.7%	10 nM ~ 0.1 mM	10 nM	[12]
Superhydrophobic surface	Drop-casting, ~hour	N.A.	75 fM ~ 75 pM	10 aM	[13]
Au NBPs/CAGB	Encapsulated the sample for direct measure, 1 minute	6.57%	1.0 nM ~ 100 μM	0.4 nM	This work

Table S3. Experimental and Reported Raman Vibrational Modes and Assignments of Uric Acid (cm^{-1})

Vibrational description	Uric acid	
	Observed	Reported[5]
Ring in-plane deformation	497	492
CO bending/skeletal ring deformation	641	634
NH bending	738	725
CN bending/in-plane ring deformation	809	811
CN stretching	1023	1016
In-plane NH bending	1208	1204
CN stretching/ in-plane NH	1354	1354
C=O stretching	1620	1653

Table S4. Comparison of the Performance of the Different SERS Platforms (Uric acid)

		Uric acid			
Ag colloid	N.A. & N.A.	8.5%	10 ~ 1000 μM	1.0 μM	[14]
Multilayered Au/Ag Substrate	N.A. & N.A.	N.A.	100 ~ 1000 μM	100 μM	[5]
Au nanoislands on the cellulose micro/nanofiber s	Dipped and dried, N.A.	N.A.	25 ~ 150 μM (in tear)	25 μM	[15]
Au nanoparticle-coated paper	Dipped and dried prior, 15 minutes	8.7% ~ 14.8%	0 ~ 3500 μM	110 μM	[16]
Au NBPs/CAGB	Encapsulated the sample for direct measure, 1 minute	N.A.	10 ~ 1000 μM	0.18 μM	This work

References

(1) Canamares, M. V.; Chenal, C.; Birke, R. L.; Lombardi, J. R., DFT, SERS, and single-molecule SERS of crystal violet. *J. Phys. Chem. C* **2008,** *112*, 20295-20300.

(2) Fu, Q.; Zhan, Z.; Dou, J.; Zheng, X.; Xu, R.; Wu, M.; Lei, Y., Highly reproducible and sensitive SERS substrates with Ag inter-nanoparticle gaps of 5 nm fabricated by ultrathin aluminum mask technique. *ACS Appl. Mater. Inter.* **2015,** *7*, 13322-13328.

(3) Lee, H. K.; Lee, Y. H.; Koh, C. S. L.; Phan-Quang, G. C.; Han, X.; Lay, C. L.; Sim, H. Y. F.; Kao, Y.-C.; An, Q.; Ling, X. Y., Designing surface-enhanced Raman scattering (SERS) platforms beyond hotspot engineering: emerging opportunities in analyte manipulations and hybrid materials. *Chemical Society Reviews* **2019,** *48*, 731-756.

(4) Kudelski, A., Raman studies of rhodamine 6G and crystal violet sub-monolayers on electrochemically roughened silver substrates: Do dye molecules adsorb preferentially on highly SERS-active sites? *Chemical Physics Letters* **2005,** *414*, 271-275.

(5) Zhao, L.; Blackburn, J.; Brosseau, C. L., Quantitative detection of uric acid by electrochemical-surface enhanced Raman spectroscopy using a multilayered Au/Ag substrate. *Analytical chemistry* **2015,** *87*, 441-447.

(6) Qiu, H.; Wang, M.; Jiang, S.; Zhang, L.; Yang, Z.; Li, L.; Li, J.; Cao, M.; Huang, J., Reliable molecular trace-detection based on flexible SERS substrate of graphene/Ag-nanoflowers/PMMA. *Sensor. Actuat. B-Chem.* **2017,** *249*, 439-450.

(7) Qian, Y.; Meng, G.; Huang, Q.; Zhu, C.; Huang, Z.; Sun, K.; Chen, B., Flexible membranes of Ag-nanosheet-grafted polyamide-nanofibers as effective 3D SERS substrates. *Nanoscale* **2014,** *6*, 4781-4788.

(8) Fusco, Z.; Bo, R.; Wang, Y.; Motta, N.; Chen, H.; Tricoli, A., Self-assembly of Au nano-islands with tuneable organized disorder for highly sensitive SERS. *J. Mater. Chem. C* **2019,** *7*, 6308-6316.

(9) Bai, S.; Serien, D.; Hu, A.; Sugioka, K., 3D microfluidic Surface‐Enhanced Raman Spectroscopy (SERS) chips fabricated by all‐femtosecond‐laser‐processing for real‐time sensing of toxic substances. *Advanced Functional Materials* **2018,** *28*, 1706262.

(10) Wang, J.; Qiu, C.; Mu, X.; Pang, H.; Chen, X.; Liu, D., Ultrasensitive SERS detection of rhodamine 6G and p-nitrophenol based on electrochemically roughened nano-Au film. *Talanta* **2020,** *210*, 120631.

(11) Kim, K.; Han, H. S.; Choi, I.; Lee, C.; Hong, S.; Suh, S.-H.; Lee, L. P.; Kang, T., Interfacial liquid-state surface-enhanced Raman spectroscopy. *Nat. Commun.* **2013,** *4*, 1-9.

(12) Huang, J.-A.; Zhang, Y.-L.; Zhao, Y.; Zhang, X.-L.; Sun, M.-L.; Zhang, W., Superhydrophobic SERS chip based on a Ag coated natural taro-leaf. *Nanoscale* **2016,** *8*, 11487-11493.

(13) De Angelis, F.; Gentile, F.; Mecarini, F.; Das, G.; Moretti, M.; Candeloro, P.; Coluccio, M.; Cojoc, G.; Accardo, A.; Liberale, C., Breaking the diffusion limit with super-hydrophobic delivery of molecules to plasmonic nanofocusing SERS structures. *Nat. Photonics* **2011,** *5*, 682-687.

(14) Westley, C.; Xu, Y.; Thilaganathan, B.; Carnell, A. J.; Turner, N. J.; Goodacre, R., Absolute quantification of uric acid in human urine using surface enhanced Raman scattering with the standard addition method. *Analytical chemistry* **2017,** *89*, 2472-2477.

(15) Park, M.; Jung, H.; Jeong, Y.; Jeong, K.-H., Plasmonic schirmer strip for human tear-based gouty arthritis diagnosis using surface-enhanced Raman scattering. *ACS nano* **2017,** *11*, 438-

443.

(16) Villa, J. E.; Poppi, R. J., A portable SERS method for the determination of uric acid using a paper-based substrate and multivariate curve resolution. *Analyst* **2016,** *141*, 1966-1972.